Estimation of Primary Quantization Steps in Double-Compressed JPEG Images Using a Statistical Model of Discrete Cosine Transform

Thanh Hai Thai, Rémi Cogranne

Date of publication xxxx 00, 0000, date of current version xxxx 00, 0000.

Digital Object Identifier 10.1109/ACCESS.2019.DOI

Estimation of Primary Quantization Steps in Double-Compressed JPEG Images Using a Statistical Model of Discrete Cosine Transform

THANH HAI THAI[1], RÉMI COGRANNE[2] (Member, IEEE)

[1]Institute of Research and Development, Duy Tan University, Da Nang, Viet Nam (email: thanhhai6587@gmail.com)

[2]Laboratory of System Modeling and Dependability, ICD - CNRS FRE 2019, Troyes University of Technology, 10004 Troyes, France (email: remi.cogranne@utt.fr).

Corresponding author: Thanh Hai Thai (e-mail: thanhhai6587@gmail.com).

This work was supported by the Conseil Régional de Champagne-Ardenne, the Grand Troyes County and the European Regional Development Fund under the program Cybersec of University of Technology of Troyes.

ABSTRACT

Double compression of images occurs when one compresses twice, possibly with different quality factors, a digital image. Estimation of the first compression parameter of such a double compression is of a crucial interest for image forensics since it may help revealing, for instance, the software or the source camera.

This paper proposes an accurate method for estimating the primary quantization steps in double-compressed JPEG images. This original methodology is based on an accurate statistical model of Discrete Cosine Transform (DCT) coefficients that has been proposed in our previous works. We also present a thorough analysis of the double compression properties, carefully taking into account carefully the effect of round-off noise. This analysis is used to derive an accurate range of possible value for quantization of primary DCT coefficients with respect to the secondary quantization step.

Using both the statistical model of quantized DCT coefficients and the range of possible values of first quantization step, a model of the twice quantized DCT coefficients is established. Eventually, it is proposed to estimate the primary quantization value by finding, among a set of possible candidates, the one that best match the proposed statistical model in terms of minimal symmetrized Kullback-Leibler (KL) divergence.

Numerical experiments on large databases of real images and comparisons with state-of-the-art approaches emphasize the relevance of the proposed method.

INDEX TERMS

Digital image forensics, Double JPEG compression, Quantization step estimation, Statistical image model, DCT coefficient analysis.

I. INTRODUCTION

THE evolution of digital imaging and information technologies in the past decades has raised a number of information security challenges. Digital images can be easily edited, altered or falsified due to a large availability of low-cost image editing tools and then transmitted via communication network. The credibility and trustworthiness of digital images have been eroded in consequence. Therefore, the field of digital image forensics has emerged in response to the increasing need to verify the authenticity of digital images, see [1] and references therein for a detailed introduction.

The JPEG standard is by far the most commonly used image format for image storage due to its rather good tradeoff between efficiency in data compression, quality and low computational costs. Hence, JPEG images are involved in many forensics issues, such as authenticity of JPEG compression history [2], steganalysis [3] or image forgery detection [4]. Recently, some research works have been paid more attention on forensics issues related to double JPEG compression [4]–[9]. In fact, double JPEG compression occurs when an image that has been previously JPEG compressed goes through a second cycle of JPEG compression. Since JPEG image is

commonly the output of most digital cameras, if a forger carries out some acts of manipulation (e.g. splicing, data hiding) on the original JPEG image and stores it in JPEG format, then the resulting image is JPEG double-compressed. Therefore, the information about double JPEG compression is of important interest for forensic analysts since it could be a clue indicating that the image in question might have been manipulated.

A. STATE OF THE ART

The problem of double JPEG compression typically includes two tasks: detection of double JPEG compression [4], [6], [9]–[12] and estimation of primary quantization matrix [4]–[8], [10]. The estimation of primary quantization matrix can be considered as a subsequent and complementary task of the double compression detection. Indeed, detection of double compressed images being usually much simpler on a computational point of view, performing detection and then, only for images classified as double compressed, carry out an estimation of primary quantization matrix would largely reduce computational time. In addition, it can be useful for forensic analysis, once suspecting that an inspected image has been double-compressed, to estimate the primary quantization matrix as such an estimation can be used to identify origin of the image [13], to detect hidden message [6] and to help image forgery detection [4]. However, the estimation of primary quantization matrix is generally more difficult and complicated than the double compression detection. The latter problem only focuses on finding discriminative features between single and double compression while the former needs to analyze the effect of double compression on DCT coefficients and carry out an exhaustive search to provide an estimate of primary quantization matrix. Moreover the detection of double JPEG compression can be carried out using together all DCT coefficient modes ; on the opposite, estimation of primary quantization step can only rely on DCT coefficients from the corresponding frequency. Therefore, compared with the detection of double compression, much fewer methods have been proposed for estimation of primary quantization matrix in the literature.

Prior research works dedicated to the estimation of primary quantization matrix could be divided into three categories:

1) Pattern-based methods [5], [6] are based on peculiarities in the shape of the histogram of DCT coefficients (e.g. double peaks, zeros) due to double compression. In [5], the authors discussed three methods to estimate primary quantization steps for the first three low-frequencies in zig-zag order. Two of them relied on matching the original histograms of individual DCT coefficients with the histograms obtained by calibration while the third one utilized a collection of neural networks to detect patterns caused by different combinations of primary and secondary quantization steps. Empirical results have shown that the neural network-based method provided best overall performances among those three. Using a very similar approach also based on the shape of histograms of DCT coefficients the authors in [6] proposed to employ, instead of neural networks, a soft-margin Support Vector Machine (SVM) to train multi-class classifiers in order to estimate primary quantization steps for the first nine low-frequencies in zig-zag order. However, these methods focused only on some small values of primary and secondary quantization steps. Hence, they could not work for high frequencies or low quality factors.
2) Quantization-based methods [7], [8] rely on properties of successive quantizations to detect local minima in the difference of DCT coefficients before and after successive quantizations, which is called the error function. In [7], the author proposed to perform a third JPEG compression on the double-compressed image under investigation. By varying the quantization step of this compression, the error function would lead to two local minima corresponding to primary and secondary quantization steps. Partially inspired by this approach, the authors in [8] proposed a strategy of filtering to mimic the effect of noise in the histogram of DCT coefficients and designed another error function devoted for good localization of primary quantization steps. However, these approaches only worked when the secondary quality factor is higher than the primary.
3) Model-based methods [4], [10] employ a statistical model of DCT coefficients for estimation of primary quantization steps. In [10], the authors proposed to model the distribution of the first digits of quantized DCT coefficients by the generalized Benford's law and employ probabilities of the first digits as features to train multiclassifiers based on Fisher Linear Discriminant (FLD) in order to estimate the primary quality factor. Alternatively, the authors in [4] proposed a heuristic model of double-quantized coefficients and estimated primary quantization steps using the expectation-maximization algorithm. While the statistical modeling of DCT coefficients has been considerably studied in the literature (see for instance [14]–[16] and references therein), those models have not been used in the previously mentioned methods for primary quantization step estimation. As a consequence, those methods fail to capture coefficients statistics with high precision which leads to the degradation of ensuing quantization step estimation accuracy. Moreover, the method proposed in [4] obtained unsatisfactory performance in case of secondary quality factor lower than the primary.

The method proposed in the present paper falls within the third category. It is based on the state-of-the-art statistical model proposed in [16]. This model is used together with a study of quantization and impact to propose a statistical model of double JPEG-compressed image DCT coefficients. Based on this model and on the impact of quantization a

method is proposed for estimating with high accuracy the primary quantization step by, roughly speaking, searching for the quantization step that would result in a distribution of DCT coefficients that best matches the empirical distribution of coefficients from the inspected image.

B. POSITION AND CONTRIBUTIONS OF THE PAPER

The present paper addresses the problem of estimation of primary quantization steps in double-compressed JPEG images assuming that secondary quantization table is available in JPEG header and the double JPEG-compressed image is available. The main contributions of this paper are the following:

- In contrast with prior statistical model-based methods, this paper proposes to exploit the state-of-the-art statistical model of once-quantized DCT coefficients that has been established in our previous works [16]–[18]. This model can accurately capture statistics of DCT coefficients, which leads to improve considerably the estimation accuracy.
- The effect of quantization in the spatial domain, when converting a JPEG-compressed image back into the original spatial domain, has often been omitted from prior-art methods for simplicity. However the resulting round-off noise can heavily impact statistics of secondary DCT coefficients, hence mislead the estimation algorithm. By contrast, this paper statistically analyze double JPEG compression properties and takes into account the effect of round-off noise, then establishes a proper range of values of primary DCT coefficients with respect to the secondary quantization step. Based on this range, the distribution of the secondary DCT coefficients is derived.
- The paper designs a method for estimation of primary quantization steps using the proposed model of secondary DCT coefficients. To do this, we propose a simple, yet efficient strategy to filter candidates of primary quantization step. Reducing the set of possible primary quantization step greatly simplifies the estimation which relies on minimizing the symmetrized Kullback-Leibler divergence between the observed empirical distribution of DCT coefficients and the theoretically established model. The proposed approach achieves high estimation accuracy when the primary quantization step is finer than the secondary, while most of existing methods failed is such a case. Numerical experiments on large real image databases with heterogeneous image content and differently customized compression scheme highlight the relevance of the proposed approach.

C. ORGANIZATION OF THE PAPER

The rest of the paper is organized as follows. Section II briefly describes the double JPEG compression operations. Section III recalls the statistical model of primary DCT coefficients that was established in our previous works, establishes the range of values of primary DCT coefficients with respect to a secondary quantization step and proposes the corresponding model of secondary DCT coefficients. Using this model, Section IV proposes the method for estimation of primary quantization steps. Section V presents numerical results on large real image databases. Finally, Section VI provides some discussions and concludes the paper.

Throughout this paper, we will use lower case characters, such as x to represent real and integer values and upper case (except for Greek letters) boldface characters $\mathbf{X}$ to represent matrices.

II. DOUBLE JPEG COMPRESSION CHAIN

The JPEG compression pipeline has been already detailed in several publications and books, such as [19] ; thus, the present paper only recalls the main parts of the JPEG compression that are essential to understand the proposed method. For clarity, the main steps involved in JPEG compression and decompression are recalled in Figure 1 along with the main notations used in the present paper. Besides, without loss of generality, we will also assume for simplicity that the inspected given image is in grayscale, the extension of color images is straightforward by applying the proposed method on each color channel independently. Let us denote $\mathbf{X}$ the original uncompressed image; the JPEG compression algorithm starts by dividing the image $\mathbf{X}$ into blocks of fixed size of 8×8 pixels [1] and performing the DCT operation on each block separately:

$$\mathbf{U}_1 = \mathrm{DCT}(\mathbf{X}). \tag{1}$$

In the paper $\mathbf{U}_1$ denotes primary unquantized DCT coefficients. The coefficient at location $(0,0)$ in 8×8 block is called the DC coefficient (for Direct Current because it represents the mean value of the block), the remaining 63 coefficients are called the AC coefficients (for Alternating Current as they correspond to sine wave oscillations in spatial domain). As explained above, prior steps such as color space transformation and chroma subsampling are not presented for the sake of clarity. The next step is the quantization operation that simply consists in dividing each primary unquantized DCT coefficient by the corresponding quantization step extracted from the primary quantization table $\mathbf{Q}_1$ of size 8×8. The final DCT coefficient is eventually rounded to the nearest integer:

$$\mathbf{C}_1 = \mathrm{round}\left(\frac{\mathbf{U}_1}{\mathbf{Q}_1}\right), \tag{2}$$

where the above division represents the element-wise operation and $\mathbf{C}_1$ denotes primary quantized DCT coefficients. We note that for clarity and readability, the present paper describes the process for a single block because, as already explained, all the blocks are processed in exactly the same manner.

The final step of JPEG standard consists in lossless compression, generally using Huffman and Run Length Encoding

[1] In this paper, it is assumed that the size of the given image is a multiple of 8. Otherwise, the JPEG compression standard uses the padding by duplicating the very last pixels.

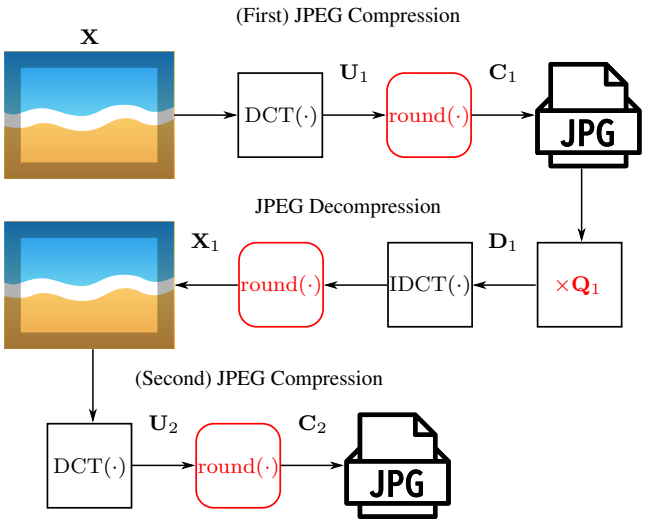

FIGURE 1: Illustration of the main steps involved in JPEG compression and decompression and used in the present work for modeling and analyzing the effect of double compression.

(RLE) ; this step of lossless compression is not detailed as it does not affect the decoded value of DCT coefficient and ensuing image pixels.

The JPEG decompression process is carried out by applying the inverse of previous operations in the reverse order, that is: "dequantization" and then inverse DCT (IDCT). Dequantization involves multiplying a primary quantized DCT coefficient by the corresponding quantization step:

$$\mathbf{D}_1 = \mathbf{C}_1 \cdot \mathbf{Q}_1, \tag{3}$$

where the above multiplication is an element-wise operation. The decompressed-JPEG image $\mathbf{X}_1$ results from applying IDCT operation on the primary dequantized DCT coefficients $\mathbf{D}_1$ to return to the spatial domain, and performing the rounding operation:

$$\mathbf{X}_1 = \text{round}\left(\text{IDCT}(\mathbf{D}_1)\right). \tag{4}$$

Though the rounding operation is not fundamentally needed (and, hence, could theoretically be avoided) it is almost always applied because most image manipulation software uses integers for better computational efficiency. Besides, it is always applied prior to the JPEG compression which is the main focus of current paper. It is important to note that quantization is the only source of loss of information during the JPEG compression. In addition, it is also important to remind that the quantization operation is used at two difference stages: first for representing quantized DCT coefficients (2) using integers, for storing purposes, and second when decompressing the image for representing pixels' value (4).

Double JPEG compression occurs when the image $\mathbf{X}_1$ suffers further JPEG compression cycle with second quantization table $\mathbf{Q}_2$:

$$\mathbf{C}_2 = \text{round}\left(\frac{\mathbf{U}_2}{\mathbf{Q}_2}\right), \text{ with } \mathbf{U}_2 = \text{DCT}(\mathbf{X}_1), \tag{5}$$

where $\mathbf{U}_2$ and $\mathbf{C}_2$ denote secondary unquantized and quantized DCT coefficients, respectively. One can observe that the rounding of pixels value, after decompression, is essential in the present analysis. Indeed, without this step one would have, from Equations (4) and (5): $\mathbf{U}_2 = \text{DCT}(\mathbf{X}_1) = \text{DCT}\left(\text{IDCT}(\mathbf{D}_1)\right) = \mathbf{D}_1$. Hence, should this statement holds true, one could decompress and recompress the same image several times with the quantization step without making any modification. This observation is well-known to be false. As already explained, rounding of pixel values before the second JPEG compression is required for two main reasons: first, because most of the image manipulation and processing softwares use integers for efficiency and (2) almost all the JPEG compression library applies the DCT from integer-value pixel to integer-value DCT because it is much more efficient computationally.

It must be noted that the present paper only focuses on the problem of aligned double JPEG compression, i.e. the second JPEG compression adopts a DCT grid aligned with the one used by the first compression [4]. The problem of non-aligned double JPEG compression is beyond the scope of the paper. From the secondary quantized DCT coefficients $\mathbf{C}_2$, one can apply the decompression process to obtain the decompressed image $\mathbf{X}_2$.

III. STATISTICAL ANALYSIS AND MODELING OF DOUBLE JPEG COMPRESSION

Images in spatial domain are usually modeled statistically using the well-known additive white Gaussian (AWG) model. However, it is well-known, especially in the field of digital image forensics, that the noise variance is slightly different for each pixel. Such differences in pixels noise variance has been successfully used for instance in source camera identification [20], [21].

The methods presented in the present paper found its root in the heteroscedastic pixel noise model [22], [23] that, taking into account photon counting shot noise, related the expectation of pixels value with their variance.

The extension of the heteroscedastic noise model of DCT coefficient of JPEG image has been studied, see for instance [24]–[26], and is briefly recalled because the present paper is based on this model. Then, this model is extended to study and model double JPEG-compressions.

A. STATISTICAL MODEL OF PRIMARY DCT COEFFICIENTS

Let u_1 and c_1 be random variables representing respectively primary unquantized and quantized DCT coefficients at a frequency. In this paper, DCT coefficients at each frequency are processed separately. For simplicity, the index of frequency is omitted. Based on the heteroscedastic model of uncompressed images X_1, the statistical model of primary unquantized and quantized DCT coefficients has been already proposed in our previous works. The reader is thus referred to [16]–[18] for details and for more justifications.

In order to account for the non-stationarity and heterogeneity in a natural image, the primary unquantized DCT coefficient u_1 can be characterized by the doubly stochastic model as [16], [17]:

$$u_1 \sim \mathcal{N}\big(0, \sigma^2\big), \text{ with } \sigma^2 \sim \mathcal{G}(\alpha, \beta), \tag{6}$$

where $\mathcal{N}\big(\mu, \sigma^2\big)$ represents the normal distribution, with μ the expected value and σ^2 the variance of the block of 8×8 pixels, $\mathcal{G}(\alpha, \beta)$ denotes Gamma distribution with shape parameter α and scale parameter β. As originally proposed in the well-known paper [15], the above doubly stochastic model allows the characterizing of probability density function (pdf) f_{u_1} of the primary unquantized DCT coefficient u_1 using the theorem of total probability:

$$f_{u_1}(z) = \sqrt{\frac{2}{\pi}} \frac{\left(|z|\sqrt{\frac{\beta}{2}}\right)^{\alpha-\frac{1}{2}}}{\beta^{\alpha}\Gamma(\alpha)} K_{\alpha-\frac{1}{2}}\left(|z|\sqrt{\frac{2}{\beta}}\right), \tag{7}$$

where $\Gamma(\cdot)$ denotes the gamma function and K_ν denotes the modified Bessel function of second kind of order ν [27]. This model includes Laplacian model as special case (as $\alpha = 1$) and Gaussian model as limiting case (as $\alpha \to \infty$).

The statistical model of the primary quantized DCT coefficient c_1 is established by taking into account the impact of quantization operation with quantization step q_1 [16], [18]. The probability mass function (pmf) P_{c_1} of the quantized DCT coefficient c_1 is given by

$$\begin{aligned} P_{c_1}(k) &= \mathbb{P}\big[c_1 = k\big] \\ &= \begin{cases} F\big(|k|\big) - F\big(|k|-1\big) & \forall k \in \mathbb{Z}_* \\ 2F(0) & k = 0, \end{cases} \end{aligned} \tag{8}$$

where $\mathbb{P}\big[A\big]$ denotes the probability of occurrence of the event A, and

$$\begin{aligned} F(k) = \frac{1}{2} g(k) \Big[& K_{\alpha-\frac{1}{2}}(g(k)) L_{\alpha-\frac{3}{2}}(g(k)) \\ & + K_{\alpha-\frac{3}{2}}(g(k)) L_{\alpha-\frac{1}{2}}(g(k)) \Big], \end{aligned} \tag{9}$$

with $g(k) = q_1(k + \frac{1}{2})\sqrt{\frac{2}{\beta}}$ and $L_\nu(\cdot)$ is the modified Struve function [27].

Maximum Likelihood (ML) estimation of the model parameters (α, β) from unquantized and quantized DCT coefficients has been also proposed in [16], [28]. As noted above, the proposed model of DCT coefficients is complicated, establishing analytically ML estimates of the parameters is hardly possible. We have proposed to resolve the problem by using numerical optimization method [29].

B. RANGE OF PRIMARY DCT COEFFICIENTS WITH RESPECT TO SECONDARY QUANTIZATION STEP

As noted in Equations (3)- (4), due to the rounding operation in spatial domain the decompression process adds round-off noise in the image $\mathbf{X}_1$:

$$\mathbf{X}_1 = \text{round}\left(\text{IDCT}(\mathbf{C}_1\mathbf{Q}_1)\right) = \text{IDCT}(\mathbf{C}_1\mathbf{Q}_1) + \boldsymbol{\xi}, \tag{10}$$

where $\boldsymbol{\xi}$ represents the random variables (matrix) that represent the quantization noise: $\boldsymbol{\xi} = \text{round}(\text{IDCT}(\mathbf{C}_1\mathbf{Q}_1)) - \text{IDCT}(\mathbf{C}_1\mathbf{Q}_1)$. One can easily observe that those random variable are independent because the quantization is an element-wise operation, hence, applied on each and every value independently.

Hence, when performing the DCT operation on the decompressed image $\mathbf{X}_1$ the resulting DCT coefficient u_2 is only an approximated version of the "unrounded" primary dequantized DCT coefficient d_1:

$$\begin{aligned} \mathbf{U}_2 &= \text{round}\big(\text{DCT}[\mathbf{X}_1]\big), \\ &= \text{round}\Big(\text{DCT}\Big[\text{IDCT}(\mathbf{C}_1\mathbf{Q}_1) + \boldsymbol{\xi}\Big]\Big), \\ &= \mathbf{C}_1\mathbf{Q}_1 + \text{round}\left(\text{DCT}(\boldsymbol{\xi})\right), \\ &= \mathbf{C}_1\mathbf{Q}_1 + \boldsymbol{\epsilon}, \end{aligned} \tag{11}$$

where ϵ represents the round-off error in DCT domain. To be comprehensive, we should also remind that the impact of "clipping", which occurs when values exceed the quantizer bounds, is assumed to be negligible in this paper. Indeed, in a vast majority of the case, pixels with values over 255 are saturated, or over-exposed, and hence belong to blocks in which pixels value is constant. In such cases all the AC (Alternative Current) DCT coefficients will be zero. As already noted in prior works, see for instance [2], [30], excluding blocks, in the image, with saturated pixels allows removing the difficulties related to clipping.

In what follows, for clarity of presentation and easy of understanding, we will present the method element-wise, and not block-wise. Hence we will use the same variable in lower case and not-boldface font to represent values of elements from previous matrices.

Due to the round-off error ϵ, the secondary unquantized DCT coefficient u_2 would cluster around integer multiples of the quantization step q_1. It is widely admitted that, when the quantization step is rather small, that the rounding noise ξ can be modeled as a uniformly distributed random variables in the interval $[-\frac{1}{2}, \frac{1}{2})$. As a consequence, the rounding error ϵ in the DCT domain can be modeled as a linear combination of spatial-domain round-off errors. In virtue of Central Limit Theorem (CLT), it is proposed in the present paper to model the error ϵ as random variable following a Gaussian distribution with zero-mean and variance of $\frac{1}{12}$ [2], [30]:

$$\epsilon \sim \mathcal{N}\left(0, \frac{1}{12}\right). \tag{12}$$

Consequently, it follows from Eq. (5) and (11), that the secondary quantized DCT coefficient c_2 can be rewritten as:

$$c_2 = \text{round}\left(\frac{c_1 q_1 + \epsilon}{q_2}\right). \tag{13}$$

By using properties of the rounding, ceiling and floor function, we can define the range of values of the primary dequantized DCT coefficient $d_1 = c_1 q_1$ as in the following Proposition:

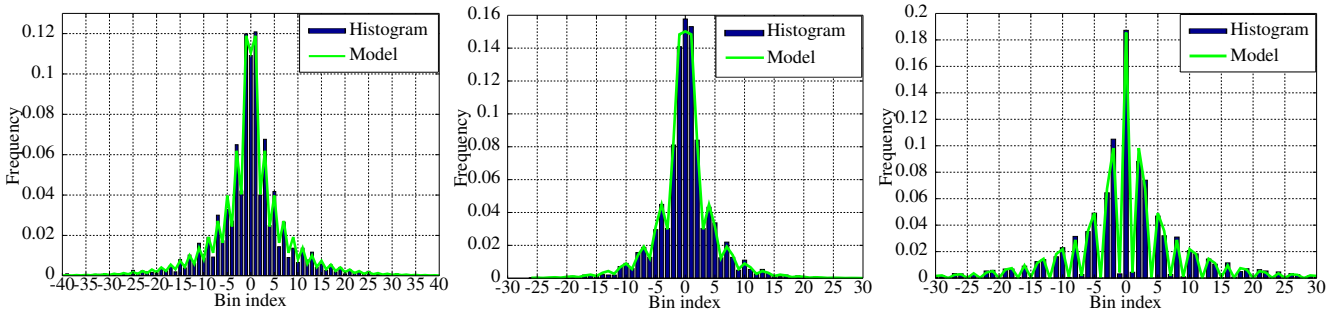

(a) $q_1 = 4, q_2 = 6$ (b) $q_1 = 6, q_2 = 10$ (c) $q_1 = 8, q_2 = 5$

FIGURE 2: Illustration of the proposed model of secondary quantized DCT coefficients on the image *Lena* with different pairs of quality factors $(\mathrm{QF}_1, \mathrm{QF}_2) = (85, 75), (75, 60), (65, 80)$. The example presented in those figures is the distribution of DCT coefficient at location $(2, 2)$ for which the quantization steps for both the quality factors QF_1 and QF_2) respectively are given as q_1 and q_2.

Proposition 1. *For a given secondary quantization step q_2 and secondary quantized DCT coefficient c_2, the value of the corresponding primary dequantized DCT coefficient d_1 falls into the range $\mathcal{R}_{q_2}(c_2)$, defined as:*

$$\mathcal{R}_{q_2}(c_2) = \left[c_2q_2 - \left\lfloor \frac{q_2}{2} + \epsilon \right\rfloor \, , \, c_2q_2 + \left\lceil \frac{q_2}{2} - \epsilon \right\rceil - 1\right], \quad (14)$$

where $\lceil x \rceil$ and $\lfloor x \rfloor$ denote the ceiling and floor function, respectively.

Proof: The proof of Proposition 1 is given in Appendix. ■

Depending on the parity of q_2, let us study the range $\mathcal{R}_{q_2}(c_2)$ in two following cases:

• **Case 1**: $q_2 = 2m, m \in \mathbb{Z}$

From (14), the range $\mathcal{R}_{q_2}(c_2)$ can be rewritten as:

$$\begin{aligned}\mathcal{R}_{q_2}(c_2) &= \left[c_2q_2 - m - \lfloor \epsilon \rfloor \, , \, c_2q_2 + m + \lceil -\epsilon \rceil - 1\right] \\ &= \left[c_2q_2 - m - \lfloor \epsilon \rfloor \, , \, c_2q_2 + m - \lfloor \epsilon \rfloor - 1\right]. \quad (15)\end{aligned}$$

It follows from (12) that the probability that the error ϵ lies outside the interval $[-\frac{3}{2}, \frac{3}{2}]$ is negligible[2]. Therefore, depending on the value of ϵ, the range $\mathcal{R}_{q_2}(c_2)$ is reduced to:

$$\begin{cases} \mathcal{R}^{(1)}_{q_2}(c_2) = \left[c_2q_2 - m + 2 \, , \, c_2q_2 + m + 1\right] & \text{if } \epsilon \in I^{(1)} \\ \mathcal{R}^{(2)}_{q_2}(c_2) = \left[c_2q_2 - m + 1 \, , \, c_2q_2 + m\right] & \text{if } \epsilon \in I^{(2)} \\ \mathcal{R}^{(3)}_{q_2}(c_2) = \left[c_2q_2 - m \, , \, c_2q_2 + m - 1\right] & \text{if } \epsilon \in I^{(3)} \\ \mathcal{R}^{(4)}_{q_2}(c_2) = \left[c_2q_2 - m - 1 \, , \, c_2q_2 + m - 2\right] & \text{if } \epsilon \in I^{(4)} \end{cases} \quad (16)$$

where $I^{(1)} = [-\frac{3}{2}, -1[$, $I^{(2)} = [-1, 0[$, $I^{(3)} = [0, 1[$, $I^{(4)} = [1, \frac{3}{2}]$.

• **Case 2**: $q_2 = 2m + 1, m \in \mathbb{Z}$

In this case, the range $\mathcal{R}_{q_2}(c_2)$ is rewritten as:

$$\mathcal{R}_{q_2}(c_2) = \left[c_2q_2 - m - \left\lfloor \epsilon + \frac{1}{2} \right\rfloor \, , \, c_2q_2 + m - \left\lfloor \epsilon - \frac{1}{2} \right\rfloor - 1\right]. \quad (17)$$

[2]The exact probably that $\epsilon \in [-\frac{3}{2}, \frac{3}{2}]$ is $2 \times \Phi(3\sqrt{3}) \approx 2.10^7$.

Similarly, the range $\mathcal{R}_{q_2}(c_2)$ can be reduced to:

$$\begin{cases} \mathcal{R}^{(1)}_{q_2}(c_2) = \left[c_2q_2 - m + 1 \, , \, c_2q_2 + m + 1\right] & \text{if } \epsilon \in I^{(1)} \\ \mathcal{R}^{(2)}_{q_2}(c_2) = \left[c_2q_2 - m \, , \, c_2q_2 + m\right] & \text{if } \epsilon \in I^{(2)} \\ \mathcal{R}^{(3)}_{q_2}(c_2) = \left[c_2q_2 - m - 1 \, , \, c_2q_2 + m - 1\right] & \text{if } \epsilon \in I^{(3)} \end{cases} \quad (18)$$

where $I^{(1)} = [-\frac{3}{2}, -\frac{1}{2}[$, $I^{(2)} = [-\frac{1}{2}, \frac{1}{2}[$, $I^{(3)} = [\frac{1}{2}, \frac{3}{2}]$.

In the literature, the round-off error ϵ is often omitted to simplify the range $\mathcal{R}_{q_2}(c_2)$. However, as noted in above analysis, due to its variability, the error ϵ impact considerably the range $\mathcal{R}_{q_2}(c_2)$. Moreover, the probability that a value falls in the sub-range $\mathcal{R}^{(j)}_{q_2}(c_2)$ equals to the one that the error ϵ is in the corresponding interval $I^{(j)}$. Therefore, the values in the range $\mathcal{R}_{q_2}(c_2)$ do not occur equally but with a different probability due to the variability of ϵ.

Corollary 1. *Combining all the sub-ranges $\mathcal{R}^{(j)}_{q_2}(c_2)$, $1 \leq j \leq n$, the range $\mathcal{R}_{q_2}(c_2)$ can be given as:*

$$\mathcal{R}_{q_2}(c_2) = \left[c_2q_2 - \left\lfloor \frac{q_2}{2} \right\rfloor - 1 \, , \, c_2q_2 + \left\lfloor \frac{q_2}{2} \right\rfloor + 1\right]. \quad (19)$$

Proof: From above analysis, by taking the minimum of left bounds and the maximum of right bounds of all the sub-ranges, the proof of Corollary 1 is straightforward. ■

Corollary 2. *Let p_j, $1 \leq j \leq n$, be the probability that the error ϵ is in the interval $I^{(j)}$, and $\bar{p}(k)$ represents the probability that the value k occurs in the range $\mathcal{R}_{q_2}(c_2)$. Then, the probability $\bar{p}(k)$ can be expressed as:*

$$\bar{p}(k) = \sum_{j=1}^{n} \mathbf{1}\left[k \in \mathcal{R}^{(j)}_{q_2}(c_2)\right] \cdot p_j, \quad (20)$$

where $\mathbf{1}[A]$ denotes the indicator function of an event A.

Proof: Since the probability that the value k occurs in the range $\mathcal{R}_{q_2}(c_2)$ equals to a sum of probabilities of occurrence of the value k in each sub-range, the proof of Corollary 2 follows immediately. ■

C. STATISTICAL MODEL OF SECONDARY DCT COEFFICIENTS

The analysis of round-off effect on the range of primary DCT coefficients allows us to establish an accurate model of secondary DCT coefficients. Let P_{C_2} denote the pmf of the random variable C_2 representing secondary quantized DCT coefficient. Based on the law of total probability, the pmf P_{C_2} can be given as:

$$\begin{aligned} P_{C_2}(c_2) &= \mathbb{P}\Big[C_2 = c_2\Big] \\ &= \sum_{k\in\mathcal{R}_{q_2}(c_2)\,,\,k=q_1 l} \mathbb{P}\Big[k\Big|C_2 = c_2\Big]\cdot\mathbb{P}\Big[D_1 = k\Big] \\ &= \sum_{k\in\mathcal{R}_{q_2}(c_2)\,,\,k=q_1 l} \mathbb{P}\Big[k\Big|C_2 = c_2\Big]\cdot\mathbb{P}\Big[C_1 = l\Big]. \end{aligned} \tag{21}$$

In other words, only multiples of q_1 in the range $\mathcal{R}_{q_2}(c_2)$ are taken into account in order to calculate the probability $P_{C_2}(c_2)$. Finally, we derive that

$$P_{C_2}(c_2) = \sum_{k\in\mathcal{R}_{q_2}(c_2)\,,\,k=q_1 l} \bar{p}(k)\cdot P_{C_1}(l). \tag{22}$$

Therefore, from the model of primary quantized DCT coefficient C_1 given in (8), the model of secondary quantized DCT coefficient C_2 can be established straightforwardly.

In order to show the efficiency of the proposed model of secondary quantized DCT coefficients, an experiment is conducted on the image Lena[3] with different pairs of quality factors $(\mathrm{QF}_1, \mathrm{QF}_2) = (85,75),(75,60),(65,80)$. Figure 2 shows the histogram of secondary quantized DCT coefficients at frequency (1,0) with corresponding quantization steps compared with the proposed model. It is noted that the proposed model can capture accurately the statistics of secondary quantized DCT coefficients, even capture specific artifacts in the histogram such as double peaks or zeros (see [5], [6] for details about those artifacts).

IV. ESTIMATION OF PRIMARY QUANTIZATION STEP

A. FILTERING OF CANDIDATES OF PRIMARY QUANTIZATION STEP

Since q_1 is a discrete integer parameter, a common philosophy is to carry out an estimation algorithm over a set of integers to provide the best candidate following certain criteria. However, in order to avoid conducting an exhaustive search, we propose a simple technique to filter possible candidates of primary quantization step q_1.

Proposition 2. *For every $c_2 \in \mathcal{C}_2$, where $\mathcal{C}_2$ denotes the set of values of secondary quantized DCT coefficients, there always exists a corresponding c_1 whose dequantized value $c_1 q_1$ is in the range $\mathcal{R}_{q_2}(c_2)$.*

[3]The reference image *Lena* can be downloaded, for instance, from https://www.ece.rice.edu/~wakin/images/.

Proof: Since $\mathcal{R}_{q_2}(c_2)$ is the range containing possible values $c_1 q_1$ with respect to the given value c_2, the Proposition 2 is straightforward. ■

Let $\kappa_{c_2}(q)$ be the function of q with respect to a coefficient c_2 defined as follows:

$$\begin{aligned} \kappa_{c_2}(q) &= \mathbf{1}\Big[\exists k\in\mathbb{Z}\mid kq\in\mathcal{R}_{q_2}(c_2)\Big] \\ &= \begin{cases} 1 & \text{if } \exists k\in\mathbb{Z} \text{ such as } kq\in\mathcal{R}_{q_2}(c_2) \\ 0 & \text{if not.} \end{cases} \end{aligned} \tag{23}$$

Then, we define the function $\bar{\kappa}(q)$ as the normalized sum of all functions $\kappa_{c_2}(q)$ for all coefficients $c_2 \in \mathcal{C}_2$:

$$\bar{\kappa}(q) = \frac{\sum_{c_2\in\mathcal{C}_2}\kappa_{c_2}(q)}{N}, \tag{24}$$

where N is the cardinality of the set $\mathcal{C}_2$, i.e. the number of secondary quantized DCT coefficients at a frequency of the image in question. Let $\mathcal{S}$ denote the set of candidates of q_1. Perfectly, the set $\mathcal{S}$ could be given as

$$\mathcal{S} = \left\{q\in\mathbb{Z}_* \,\middle|\, \bar{\kappa}(q) = 1\right\}. \tag{25}$$

The proposed filtering technique is illustrated in Figure 3 for two scenarios $q_1 < q_2$ and $q_1 > q_2$. The DCT coefficients at the frequency (0,1) of the image Lena are used in this experiment. It could be noted that in case of $q_1 < q_2$, the true primary quantization step q_1 is included in the values smaller than q_2. Generally, the proposed technique can narrow down the search on the primary quantization step q_1, which allows to reduce considerably execution time.

In practice, the function $\bar{\kappa}(q)$ at the true primary quantization step can have value slightly lower than 1 due to the small effect of truncation errors and modeling error of ϵ [2], [28]. Therefore, the set of candidates $\mathcal{S}$ is proposed as follows:

$$\mathcal{S} = \left\{q\in\mathbb{Z}_* \,\middle|\, \bar{\kappa}(q) \geq 0.9\right\}. \tag{26}$$

B. PROPOSED ESTIMATION ALGORITHM

After establishing the candidate set $\mathcal{S}$, this paper provides the optimal candidate based on the criteria of symmetrized KL distance. In probability and information theories, the KL divergence [31], which is an asymmetric discrepancy measure between two probability distributions P_1 and P_2, is defined as follows:

$$D_{KL}\big(P_1\|P_2\big) = \int \log\frac{\mathrm{d}P_1}{\mathrm{d}P_2}\mathrm{d}P_1. \tag{27}$$

In case of discrete probability distributions, the KL divergence $D_{KL}\big(P_1\|P_2\big)$ can be given by:

$$D_{KL}\big(P_1\|P_2\big) = \sum_i P_1(i)\log\frac{P_1(i)}{P_2(i)}. \tag{28}$$

However, it is noted that $D_{KL}\big(P_1\|P_2\big)$ is not a strict concept of distance since it does not obey the triangle inequality and it is not symmetric in general, i.e. $D_{KL}\big(P_1\|P_2\big) \neq D_{KL}\big(P_2\|P_1\big)$. Therefore, in order to quantify the similarity

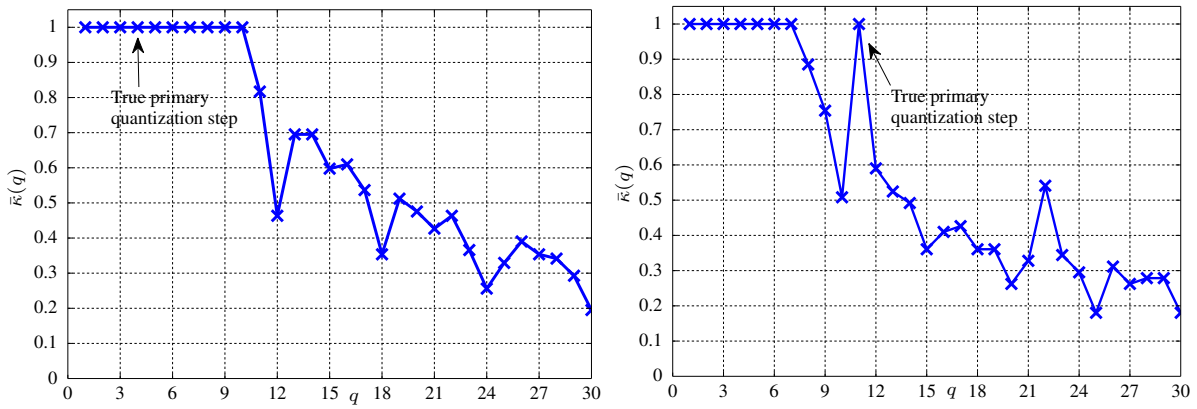

(a) $q_1 = 4, q_2 = 6$ (b) $q_1 = 11, q_2 = 5$

FIGURE 3: Illustration of the proposed technique for filtering of candidates of primary quantization step using the DCT coefficient at location $(2, 2)$ and with two examples for quality factors $(\mathrm{QF}_1, \mathrm{QF}_2) = (85, 75), (55, 80)$. As in Figure 2, the quantization steps are given by q_1 and q_2 for quality factors QF_1 and QF_2) respectively.

between two probability distributions P_1 and P_2, we rely on the symmetrized KL distance given as:

$$\overline{D}_{KL} = D_{KL}\big(P_1 \| P_2\big) + D_{KL}\big(P_2 \| P_1\big). \tag{29}$$

To provide the optimal candidate of q_1, we calculate the symmetrized KL distance between the normalized observed histogram H of secondary quantized DCT coefficients and the theoretical model P_{C_2} under a candidate $q \in \mathcal{S}$

$$\overline{D}_{KL}(q) = \sum_{|i|\geq 2} H(i) \log \frac{H(i)}{P_{C_2}(i \mid \boldsymbol{\theta})} + \sum_{|i|\geq 2} P_{C_2}(i \mid \boldsymbol{\theta}) \log \frac{P_{C_2}(i \mid \boldsymbol{\theta})}{H(i)}, \tag{30}$$

where i denotes the histogram bin index and $\boldsymbol{\theta} = (\alpha, \beta, q, q_2)$ is the parameter vector specifying the probability distribution P_{C_2}. It is noted that in the calculation of $\overline{D}_{KL}(q)$, the bin index at 0 and ± 1 are excluded. The main difficulty in (30) is that the nuisance parameters (α, β) are unknown in practice, hence the distance $\overline{D}_{KL}(q)$ could not be computed. To overcome this difficulty, it is proposed to transform the decompressed image $\mathbf{X}_2$ to the DCT domain, then estimate the parameters (α, β) from unquantized DCT coefficients by the ML method (see Section III-A). The ML estimates are then replaced in (30). Finally, the optimal candidate of primary quantization step q_1 is given as the value minimizing the symmetrized KL distance:

$$q^* = \arg\min_{q \in \mathcal{S}} \overline{D}_{KL}(q). \tag{31}$$

It should be noted that one can, in fact, estimate the quantization step by find the value that minimizes a different "metric" than the proposed asymmetric Kullback-Leibler divergence. Indeed by simply using in Eq. (31) a quantitive comparison between the theoretical distribution $P_{C_2}(i \mid \boldsymbol{\theta})$ with the empirical observation $H(i)$. We focus in the present paper on the asymmetric Kullback-Leibler divergence because, as shown in Table 1 it has been empirically observed that it provide the best results.

It is important to keep in mind that the present paper focuses on estimating an individual primary quantization step rather than a primary quality factor. This is of great interest in practice because most quantization tables used in digital cameras are often customized by camera manufacturers using their own compression scheme, despite standard quantization tables have been provided by the Independent JPEG Group [19]. Therefore, the proposed approach could partially recover the employed primary quantization table, which helps to identify the source camera model [13].

V. EXPERIMENTS

For estimation of primary quantization step, the proposed approach excludes the secondary coefficients whose absolute value is smaller than 1, see (30). When an image is highly compressed, i.e. the secondary quantization step is very coarse, all secondary coefficients could be quantized into the interval $[-1, 1]$. In this case, the estimation is declared undetermined. To the best of our knowledge, no method (including the present one) can deal with this case.

Moreover, the proposed approach could not provide reliable estimation of primary quantization steps when q_1 is a divisor of q_2 (including 1 and q_2) because the histogram in these cases is very close to the one generated from single compression, i.e. the DCT coefficients are not technically double-compressed [5], [6]. These cases would be our focus in future research.

In this paper, the performance of the method is evaluated using the accuracy metric, which is calculated as a percentage of the number of correctly estimated quantization steps.

TABLE 1: Estimation accuracy of the proposed approach for different metrics when the second quantization step is $q_2 = 8$ and for various primary quantization step $q_1 \in [1, 20]$. The various metrics used in the comparison with the proposed method (31) are respectively the symmetrized Kullback-Leibler divergence (Sym. KL), the Pearson's chi-sqaured, χ^2, the Maximum Likelihood (ML) the (asymmetric) Kullback-Leibler divergence denoted Asym. KL, the L^1-norm and the L^2-norm respectively.

(a) Simulated data

q_1	Sym. KL	χ^2	ML	Asym. KL	L^1	L^2
1	-	-	-	-	-	-
2	-	-	-	-	-	-
3	**98.05**	77.90	5.25	5.25	58.42	41.31
4	-	-	-	-	-	-
5	**98.75**	89.83	10.23	10.23	82.17	80.34
6	**99.58**	90.80	62.64	62.64	92.21	90.30
7	**99.89**	93.34	93.01	93.01	93.12	90.89
8	-	-	-	-	-	-
9	**99.90**	94.95	11.83	11.83	94.10	90.62
10	**100.00**	93.31	12.22	12.22	97.87	97.25
11	**100.00**	98.50	95.05	95.05	90.62	89.11
12	**100.00**	94.77	93.82	93.82	93.01	92.72
13	**100.00**	100.00	97.52	97.52	97.11	96.98
14	**100.00**	100.00	98.27	98.27	97.88	97.12
15	**100.00**	100.00	97.15	97.15	95.43	94.98
16	**100.00**	100.00	99.19	99.19	98.41	97.75
17	**99.93**	98.91	88.72	88.72	89.93	88.56
18	**100.00**	100.00	100.00	100.00	98.24	98.11
19	**100.00**	100.00	100.00	100.00	97.69	97.03
20	**100.00**	100.00	100.00	100.00	97.22	97.25

(b) Real data

q_1	Sym. KL	χ^2	ML	Asym. KL	L^1	L^2
1	-	-	-	-	-	-
2	-	-	-	-	-	-
3	**95.53**	65.69	2.05	2.05	59.58	40.95
4	-	-	-	-	-	-
5	**98.36**	82.39	7.45	7.45	79.11	71.66
6	**99.44**	87.46	59.32	59.32	89.01	88.18
7	**99.85**	86.60	83.79	83.79	80.57	76.93
8	-	-	-	-	-	-
9	**99.82**	88.51	4.23	4.23	93.59	89.39
10	**99.48**	90.99	4.23	4.23	97.17	95.15
11	**99.75**	96.78	94.33	94.33	88.63	88.59
12	**99.82**	93.19	93.81	93.81	90.78	90.12
13	**99.85**	99.07	96.50	96.50	95.16	95.29
14	**99.81**	99.06	97.22	97.22	96.09	95.36
15	**99.84**	99.25	96.99	96.99	94.82	94.84
16	**99.89**	99.62	97.17	97.17	95.42	95.13
17	**99.73**	96.24	87.65	87.65	88.67	85.92
18	**99.97**	99.03	98.11	98.11	95.25	94.71
19	**99.95**	99.08	98.39	98.39	94.68	92.32
20	**100.00**	99.39	98.23	98.23	93.40	93.88

A. VALIDATION OF THE PROPOSED STATISTICAL FRAMEWORK

The proposed statistical framework has shown a possibility of employing a different model of DCT coefficients (e.g. Laplacian, Generalized Gaussian or Generalized Gamma distribution) or a different metric for similarity measure. In our previous works [16], the proposed model of DCT coefficients has been already shown to outperform other models. Therefore, in this paper, we conduct experiments to validate the choice of symmetrized KL distance over different metrics.

Firstly, we conduct an experiment on simulated data. The simulated data is generated using 10000 uncompressed grayscale images of size 512×512 in the BOSSBase [32] (version 1.01). The simulation process is given as follows:

1) The experiment starts from transforming each uncompressed image in the BOSSBase into DCT domain, then estimate the parameters (α, β) from unquantized DCT coefficients at frequency (1,0).
2) From a given couple (α, β), a vector of 4096 coefficients u_1 is randomly generated following the model as in (7).
3) The coefficients u_1 are then quantized and dequantized with primary step q_1, obtained d_1.
4) The primary dequantized coefficients d_1 are added by noise ϵ following the Gaussian distribution as in (12) to create u_2.
5) The coefficients u_2 are finally quantized with secondary step q_2, obtained c_2.

By doing so, we obtain the coefficients c_2 that fit the theoretical model perfectly. Moreover, the fact of using the parameters (α, β) by estimating from a real image for simulation process could provide DCT coefficients close to reality. In this simulation, the step q_2 is fixed to $q_2 = 8$ and the step q_1 varies in the interval $[1, 20]$. The above simulation process is applied for 10000 uncompressed images in the BOSSBase. Therefore, the simulated data involves 10000 vectors of coefficients c_2 for each primary quantization step q_1. The experiment is conducted for different metrics, including the Symmetrized KL distance χ^2-distance, ML method, asymmetric KL divergence, L^1-norm and L^2-norm.

Next, we conduct a second experiment on real data, which also relies on the BOSSBase. The uncompressed images are double-JPEG compressed with constant quantization tables, where all steps in the quantization table take the same value. The primary steps vary in the interval $[1, 20]$ and the secondary ones are fixed to 8. Then DCT coefficients at frequency (1,0) are extracted for estimation. By doing so, this experiment is carried out in a similar scenario as the first one on simulated data.

The estimation accuracy of the proposed approach for different metrics on the simulated data and real data is shown in Table 1. It should be noted that the performance

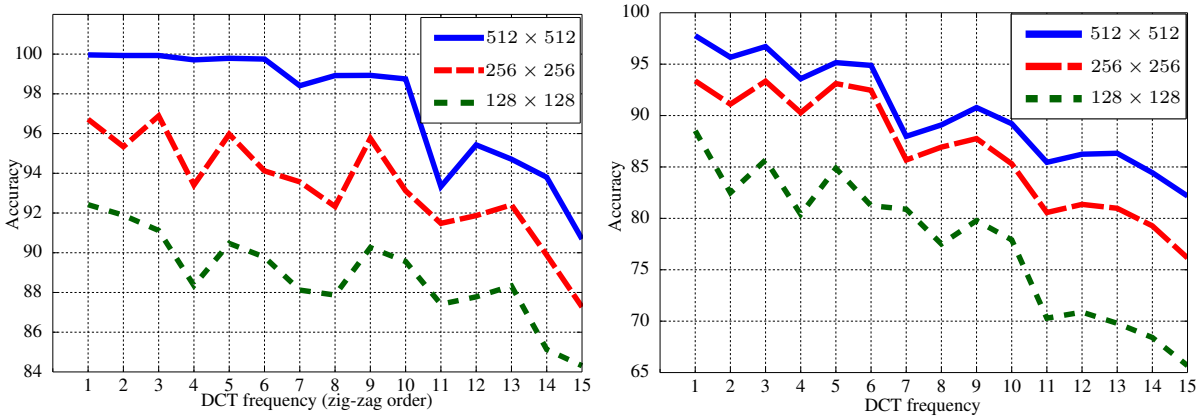

(a) $\mathrm{QF}_1 < \mathrm{QF}_2$ (b) $\mathrm{QF}_1 > \mathrm{QF}_2$

FIGURE 4: Estimation accuracy of the proposed method using one of the first 15 frequencies (in zig-zag order) of images with different sizes from the BOSSBase. The values are obtained by averaging over all $(\mathrm{QF}_1, \mathrm{QF}_2)$.

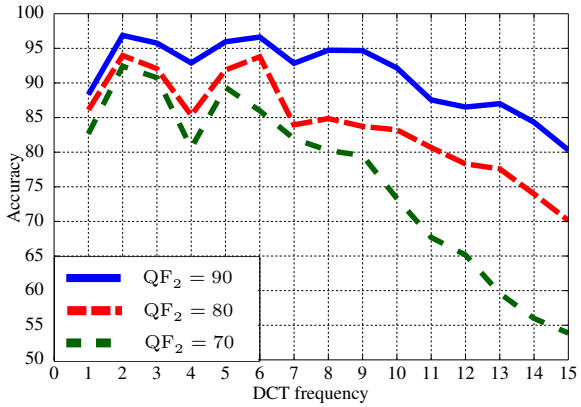

FIGURE 5: Estimation accuracy of the proposed method on the Dresden database.

for all values q_1 divisors of q_2 is not presented in this table. The proposed approach using the symmetrized KL distance achieves mostly perfect performance, which validates this choice over other metrics. The performance for other metrics is unsatisfactory when $q_1 < q_2$. Surprisingly, the proposed approach based on ML method and asymmetric KL divergence obtains the poorest performance in that case. The high performance of the proposed approach in those experiments shows that the above statistical framework is relevant to model statistics of secondary DCT coefficients. Furthermore, the proposed method can estimate accurately individual primary quantization steps in the case when the primary quantization step is finer than the secondary one.

B. NUMERICAL RESULTS ON LARGE REAL IMAGE DATABASE

In order to emphasize the effectiveness of the proposed approach, we carry out experiments on large real image databases and comparisons with existing methods. Firstly, an experiment is carried out on the BOSSBase. All 10000 grayscale uncompressed images in this database are JPEG-compressed twice using the Matlab JPEG Toolbox [33] with quality factors $\mathrm{QF}_1 \in \{60, 65, 70, 75, 80, 85, 90, 95\}$ and $\mathrm{QF}_2 \in \{60, 65, 70, 75, 80, 85, 90, 95, 100\}$. It should be noted that images from the BOSSBase have an important variability in their content. Conducting the experiment on such a large image database can allow us to assess the robustness of the estimation method. Moreover, to assess the performance for different image sizes, those 512×512 original images are center-cropped into images of size 256×256 and 128×128 before conducting double compression. Thus, the final dataset contains 720000 double-compressed images for each image size.

It is noted that the proposed approach is based on statistics of secondary DCT coefficients at each separate frequency. Due to insufficient statistics at high frequencies, the paper only focuses on studying the performance at low and medium frequencies. Table 2 shows the estimation accuracy of the proposed method at the first 10 frequencies in zig-zag order of double-compressed images of size 512×512 in the BOSSBase dataset. The column and row of Table 2 represent respectively primary and secondary quality factor. Similarly, the case in which primary step is a divisor of secondary one is not presented in this Table. These results emphasize the high performance of the proposed method when applying on real large image database. When $\mathrm{QF}_1 < \mathrm{QF}_2$ (i.e. $q_1 > q_2$), the estimation accuracy at low frequencies is nearly perfect despite high compression. For higher frequencies, it can be observed that the estimation accuracy decreases with the decline of the quality factor. Especially, when $\mathrm{QF}_1 > \mathrm{QF}_2$ (i.e. $q_1 < q_2$), the estimation accuracy tends to increase as the primary quality factor decreases. This is due to the fact that when the primary quality factor is very high, the effect of double compression is minor (i.e. the image is close to the one generated from the single compression of QF_2), hence

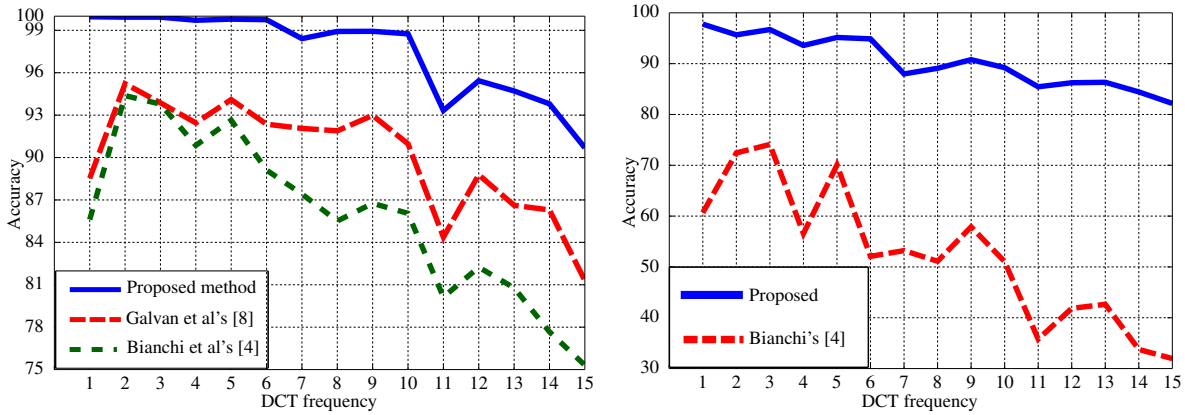

(a) $\mathrm{QF}_1 < \mathrm{QF}_2$ (b) $\mathrm{QF}_1 > \mathrm{QF}_2$

FIGURE 6: Comparison in terms of estimation accuracy between the proposed methods and prior work. The comparison has been carried out on all images from the BOSSBase with the original size of 512×512 pixels.

the proposed estimator can be mistaken.

Furthermore, the performance of the proposed method for the images with different sizes from the BOSSBase is shown in Figure 4. The estimation accuracy for various DCT coefficients (scanned using the zig-zag pattern order) in the case of $\mathrm{QF}_1 < \mathrm{QF}_2$ and $\mathrm{QF}_1 > \mathrm{QF}_2$ is reported respectively. The values in this Figure are averaged estimation accuracy considering all combinations of $(\mathrm{QF}_1, \mathrm{QF}_2)$ studied in Table 2. It can be clearly observed that the estimation accuracy of the proposed method is strictly correlated with the image size. Moreover, the decline of the performance in case $\mathrm{QF}_1 > \mathrm{QF}_2$ tends to be faster than the one in case $\mathrm{QF}_1 < \mathrm{QF}_2$.

To further confirm the effectiveness of the proposed approach, an experiment is conducted on the real JPEG image from the Dresden database [34] that is publicly available for download. This database includes 16958 color JPEG images acquired from 73 different camera devices of different models/brands with the highest available resolution and JPEG quality setting, see more details in [34]. The color JPEG compression introduces some additional steps such as color space transformation (e.g. RGB to YCbCr and inverse) and chrominance component downsampling. These steps generate noise into the color components. By conducting experiments on real color JPEG images, we do not only verify the robustness of the proposed method to color noise although it is not yet incorporated in the proposed model, but also show its effectiveness in the real JPEG compression scheme designed by different manufacturers. In this experiment, the color JPEG images are converted into grayscale and then gone through a second JPEG compression using the Matlab JPEG Toolbox [33] with quality factors $\mathrm{QF}_2 \in \{90, 80, 70\}$. The estimation accuracy of the proposed method on those double-compressed JPEG images is shown in Figure 5. It is noted that there is a drop in performance at frequency (0,0). This is due to the fact that the DC coefficient represents the average of pixel values in a block, which causes a difficulty to provide an accurate model due to high heterogeneity in a natural image. Nevertheless, the proposed method can estimate accurately the primary quantization steps at low frequencies. This highlights its practicability at recovering a part of employed quantization matrix in natural JPEG images taken by a digital camera, which could help to identify the image origin.

Considering the scenario of estimating individual primary quantization steps, the paper proposes to carry out a comparison with two recent methods, including the quantization-based method proposed by Galvan *et al.* [8] and the model-based method proposed by Bianchi *et al.* [4][4]. The comparison is conducted on the double-compressed JPEG images with size of 512×512 in the BOSSBase. The performance of all the methods is shown in Figure 6. Because Galvan's method cannot be performed in the case $\mathrm{QF}_1 > \mathrm{QF}_2$, its performance is not reported in Figure 6b. As noted, the proposed method outperforms the others in terms of estimation accuracy, especially when the primary quantization step is finer than the secondary.

VI. CONCLUSION, DISCUSSION AND FUTURE WORKS

This paper proposes an accurate method for estimation of primary quantization step in a double-compressed JPEG image. The approach is based on the statistical model of DCT coefficients that has been given in our previous works. By analyzing the double quantization effect and taking into account the round-off noise, the paper establishes an appropriate model of the secondary DCT coefficients. Moreover, by using a simple and efficient filtering technique, a set of possible candidates of primary quantization step is provided. From this set of candidates, the optimal candidate is given following the criteria of symmetrized KL distance.

[4]The Matlab code of this method has been provided at https://iapp.dinfo.unifi.it/.

Numerical experiments on large image databases highlight the relevance of the proposed approach.

The strength of the proposed method is the high estimation accuracy for a wide variety of images with different image contents, image sizes, and quality factors. Moreover, the proposed method can provide reliable estimation of primary quantization steps in the case that the primary quantization step is finer than the secondary while all the prior methods have failed. The accuracy of the proposed method is emphasized when applying on real color JPEG images acquired from different camera models/brands, which shows the robustness of the proposed method to color noise introduced during JPEG compression pipeline. However, the proposed method is more time-consuming than prior-art ones. This drawback is due to the fact that the ML estimation of DCT model parameters is accomplished using a numerical optimization method.

The approach proposed in this paper explore several directions in future researches. Firstly, based on the study of double compression effect in this paper, we could design a statistical test following hypothesis testing theory in order to detect the presence of double-JPEG compression. This test can allow the guaranteeing of a prescribed false-alarm rate, which is crucial in an operational context. It should be noted that such statistical test has not yet studied in the literature. The second research is the estimation of primary quantization steps from non-aligned double-compressed JPEG images. Last but not least, it is of crucial interest to detect and localize copy-paste forgery using inconsistencies in JPEG compression history among different parts in the image under investigation.

APPENDIX. PROOF OF PROPOSITION 1

The goal of this appendix is to provide a proof for the Proposition 1 and, more precisely, to prove Equation (14).

Let us recall that using that the image compressed only once is decompressed in spatial domain, via multiplication of coefficients c_1 with quantization step q_1, inverse DCT transformation and rounding of pixels' value. This decompressed image is then compressed a second time with a different quantization step q_2. Modeling the rounding error of pixels' value with a uniformly distributed random variable allows the writing of Equation (13):

$$c_2 = \text{round}\left(\frac{c_1 q_1 + \epsilon}{q_2}\right).$$

Based on the definition of the rounding function and on the previous relation, it immediately follows from that:

$$c_2 - \frac{1}{2} \leq \frac{c_1 q_1 + \epsilon}{q_2} < c_2 + \frac{1}{2}, \tag{32}$$

which is equivalent to:

$$c_2 q_2 - \frac{q_2}{2} - \epsilon \leq c_1 q_1 < c_2 q_2 + \frac{q_2}{2} - \epsilon, \tag{33}$$

Taking into account that c_1 and q_1 are both integers, one has:

$$\left\lceil c_2 q_2 - \frac{q_2}{2} - \epsilon \right\rceil \leq c_1 q_1 \leq \left\lceil c_2 q_2 + \frac{q_2}{2} - \epsilon \right\rceil - 1. \tag{34}$$

Therefore, we derive

$$c_2 q_2 + \left\lceil -\left(\frac{q_2}{2} + \epsilon\right) \right\rceil \leq c_1 q_1 \leq c_2 q_2 + \left\lceil \frac{q_2}{2} - \epsilon \right\rceil - 1. \tag{35}$$

Since $\lceil -x \rceil = -\lfloor x \rfloor$, we obtain:

$$c_2 q_2 - \left\lfloor \frac{q_2}{2} + \epsilon \right\rfloor \leq c_1 q_1 \leq c_2 q_2 + \left\lceil \frac{q_2}{2} - \epsilon \right\rceil - 1, \tag{36}$$

Finally, observing that the product $c_1 q_1$ is the same quantity as the corresponding primary dequantized DCT coefficient d_1, it is obvious that the previous Equation (36) corresponds to Equation (14) which concludes the proof of Proposition 1. ■

REFERENCES

[1] M. C. Stamm, M. Wu, and K. J. R. Liu, "Information forensics: An overview of the first decade," IEEE Access, vol. 1, pp. 167–200, May 2013.
[2] Z. Fan and R. Queroz, "Identification of bitmap compression history: JPEG detection and quantizer estimation," IEEE Trans. Image Process., vol. 12, no. 2, pp. 230–235, Feb. 2003.
[3] V. Holub and J. Fridrich, "Low-complexity features for JPEG steganalysis using undecimated DCT," IEEE Trans. Inf. Forensics Security, vol. 10, no. 2, pp. 219–228, Feb. 2015.
[4] T. Bianchi and A. Piva, "Image forgery localization via block-grained analysis of JPEG artifacts," IEEE Trans. Inf. Forensics Security, vol. 7, no. 3, pp. 1003–1017, Jun. 2012.
[5] J. Lukas and J. Fridrich, "Estimation of primary quantization matrix in double compressed JPEG images," in Proc. Digital Forensic Res. Workship, Aug. 2003, pp. 5–8.
[6] T. Pevny and J. Fridrich, "Detection of double compression in JPEG images for applications in steganography," IEEE Trans. Inf. Forensics Security, vol. 3, no. 2, pp. 247–258, Jun. 2008.
[7] H. Farid, "Exposing digital forgeries from jpeg ghosts," IEEE Trans. Inf. Forensics Security, vol. 4, no. 1, pp. 154–160, Mar. 2009.
[8] F. Galvan, G. Puglisi, A. Bruna, and S. Battiato, "First quantization matrix estimation from double compressed JPEG images," IEEE Trans. Inf. Forensics Security, vol. 9, no. 8, pp. 1299–1310, Aug. 2014.
[9] J. Yang, J. Xie, G. Zhu, S. Kwong, and Y. Shi, "An effective method for detecting double JPEG Compression with the same quantization matrix," IEEE Trans. Inf. Forensics Security, vol. 9, no. 11, pp. 1933–1942, Nov. 2014.
[10] B. Li, Y. Q. Shi, and J. Huang, "Detecting doubly compressed JPEG images by using mode based first digit features," in Proc. IEEE Workshop Multimedia Signal Process., Oct. 2008, pp. 730–735.
[11] F. Huang, J. Huang, and Y.-Q. Shi, "Detecting double JPEG compression with the same quantization matrix," IEEE Trans. Inf. Forensics Security, vol. 5, no. 4, pp. 848–856, Dec. 2010.
[12] T. Bianchi and A. Piva, "Detection of non aligned double JPEG compression based on integer periodicity maps," IEEE Trans. Inf. Forensics Security, vol. 7, no. 2, pp. 842–848, Apr. 2012.
[13] E. Kee, M. K. Johnson, and H. Farid, "Digital image authentication from JPEG headers," IEEE Trans. Inf. Forensics Security, vol. 6, no. 3, pp. 1066–1075, Sept. 2011.
[14] F. Muller, "Distribution shape of two-dimensional DCT coefficients of natural images," Electro. Lett., vol. 29, no. 22, pp. 1935–1936, Oct. 1993.
[15] E. Y. Lam and J. W. Goodman, "A mathematical analysis of the DCT coefficient distributions for images," IEEE Trans. Image Process., vol. 9, no. 10, pp. 1661–1666, Oct. 2000.
[16] T. H. Thai, R. Cogranne, and F. Retraint, "Statistical model of quantized DCT coefficients: Application in the steganalysis of Jsteg algorithm," IEEE Trans. Image Process., vol. 23, no. 5, pp. 1980–1993, May 2014.
[17] T. H. Thai, R. Cogranne, and F. Retraint, "Statistical model of natural images," in Proc. IEEE. Int. Conf. Image Process., Sep. 2012, pp. 2525–2528.
[18] T. H. Thai, R. Cogranne, and F. Retraint, "Steganalysis of Jsteg algorithm based on a novel statistical model of quantized DCT coefficients," in Proc. IEEE Int. Conf. Image Process., Sep. 2013, pp. 4427–4431.
[19] W. Pennebaker and J. Mitchell, JPEG Still Image Compression Data. Springer, 1992.

[20] M. Chen, J. Fridrich, M. Goljan, and J. Lukas, "Determining image origin and integrity using sensor noise," IEEE Trans. Inf. Forensics Security, vol. 3, no. 1, pp. 74–90, Mar. 2008.
[21] C.-T. Li, "Source camera identification using enhanced sensor pattern noise," IEEE Trans. Inf. Forensics Security, vol. 5, no. 2, pp. 280–287, Jun. 2010.
[22] G. E. Healey and R. Kondepudy, "Radiometric CCD camera calibration and noise estimation," IEEE Trans. Pattern Anal. Mach. Intell., vol. 16, no. 3, pp. 267–276, Mar. 1994.
[23] A. Foi, M. Trimeche, V. Katkovnik, and K. Egiazarian, "Practical Poissonian-Gaussian noise modeling and fitting for single-image raw-data," IEEE Trans. Image Process., vol. 17, no. 10, pp. 1737–1754, Oct. 2008.
[24] T. H. Thai, R. Cogranne, and F. Retraint, "Camera model identification based on the heteroscedastic noise model," IEEE Trans. Image Process., vol. 23, no. 1, pp. 250–263, Jan. 2014.
[25] T. H. Thai, F. Retraint, and R. Cogranne, "Camera model identification based on DCT coefficient statistics," Digit. Signal Process., vol. 40, pp. 88–100, May 2015.
[26] T. Qiao, F. Retraint, R. Cogranne, and T. H. Thai, "Individual camera device identification from jpeg images," Signal Processing: Image Communication, vol. 52, pp. 74 – 86, 2017.
[27] I. M. Ryzhik and I. S. Gradshteyn, Tables of Integrals, Series, and Products. United Kingdom: Elsevier, 2007.
[28] T. H. Thai, R. Cogranne, F. Retraint, and T.-N.-C. Doan, "JPEG quantization step estimation and its applications to digital image forensics," IEEE Trans. Inf. Forensics Security, vol. 12, no. 1, pp. 123–133, Jan. 2017.
[29] J. A. Nelder and R. Mead, "A simplex method for function minimization," Comput. J., vol. 7, pp. 308–313, 1965.
[30] W. Luo, J. Huang, and G. Qiu, "JPEG error analysis and its application to digital image forensics," IEEE Trans. Inf. Forensics Security, vol. 5, no. 3, pp. 480–491, Sep. 2010.
[31] S. Kullback and R. A. Leibler, "On information and sufficiency," Ann. Math. Statist., vol. 22, no. 1, pp. 79–86, Mar. 1951.
[32] P. Bas, T. Filler, and T. Pevný, "Break our steganographic system — the ins and outs of organizing boss," in Proc. Int. Workshop Inf. Hiding, May 2011.
[33] P. Sallee, "Matlab JPEG Toolbox" [online]. Available at http://dde.binghamton.edu/download/jpeg_toolbox.zip."
[34] T. Gloe and R. Bohme, "The Dresden image database for benchmarking digital image forensics," in Proc. ACM Symposium Applied Comput., vol. 2, 2010, pp. 1585–1591.

THANH HAI THAI received the Diploma, M.S. and Ph.D degrees in systems optimization and safety from the University of Technology of Troyes, in 2011 and 2014, respectively. He is currently a Researcher with the Institute of Research and Development, Duy Tan University, Da Nang, Viet Nam. His research focuses on statistical image processing, hypothesis testing theory, steganography and steganalysis, and digital image forensics.

RÉMI COGRANNE is an Associate Professor at Troyes University of Technology (UTT), France, since 2013. He has regularly been a visiting scholar at Binghamton University between 2014 and 2017. He received his PhD in Systems Safety and Optimization from UTT in 2011, since on, his research focuses on hypothesis testing applied to image forensics, steganalysis, steganography and computer network anomaly detection which lead to more than 60 papers and 3 International patents. He has been the general Chair of ACM Workshop on Information Hiding and Multimedia Security (2019), main organizer of ALASKA steganalysis challenge (https://alaska.utt.fr), Member of IEEE and Elected Member of IEEE Technical Committee Information Forensics and Security (2019âĂŞ2021)

TABLE 2: Estimation accuracy of the proposed method using each and every first ten DCT coefficients (according to the zig-zag pattern order) and over all the images in the BOSSBase with the original size of 512×512 pixels.

(a) Frequency (0,0)

	95	90	85	80	75	70	65	60
100	100.00	100.00	100.00	100.00	99.99	99.99	99.99	99.97
95	-	100.00	100.00	100.00	99.99	99.98	99.98	99.97
90	99.98	-	99.99	99.98	99.98	99.98	99.98	99.97
85	99.95	99.95	-	99.99	99.98	99.98	99.95	99.95
80	-	-	99.88	-	99.98	99.95	99.95	99.92
75	-	97.77	98.72	99.69	-	99.92	99.89	99.89
70	-	96.75	-	99.40	99.68	-	99.89	99.89
65	94.26	96.19	96.22	98.07	99.65	99.65	-	99.86
60	92.30	92.31	98.23	92.33	99.21	99.28	99.30	-

(b) Frequency (0,1)

	95	90	85	80	75	70	65	60
100	-	100.00	100.00	100.00	99.99	99.99	99.99	99.97
95	-	100.00	100.00	100.00	99.99	99.98	99.98	99.97
90	-	-	99.99	99.98	99.98	99.98	99.98	99.97
85	-	99.85	-	99.99	99.98	99.98	99.95	99.95
80	-	-	99.23	-	99.98	99.95	99.95	99.92
75	-	-	-	99.65	-	99.92	99.89	99.89
70	-	93.42	94.52	95.74	93.58	-	99.89	99.89
65	-	-	91.12	-	95.16	95.68	-	98.85
60	-	90.71	-	92.21	99.50	97.52	97.17	-

(c) Frequency (1,0)

	95	90	85	80	75	70	65	60
100	-	100.00	100.00	100.00	99.99	99.99	99.99	99.97
95	-	100.00	100.00	100.00	99.99	99.98	99.98	99.97
90	-	-	99.99	99.98	99.98	99.98	99.98	99.97
85	-	-	-	99.99	99.98	99.98	99.95	99.95
80	-	97.57	99.20	-	99.98	99.95	99.95	99.92
75	-	-	99.62	96.30	-	99.92	99.89	99.89
70	-	93.33	94.52	99.58	99.05	-	99.89	99.89
65	-	-	-	95.83	96.93	95.06	-	98.86
60	-	-	92.43	-	96.84	96.77	97.73	-

(d) Frequency (2,0)

	95	90	85	80	75	70	65	60
100	-	100.00	99.99	99.97	99.97	99.95	99.95	99.93
95	-	99.99	99.93	99.90	99.90	99.90	99.84	99.84
90	-	-	99.82	99.80	99.81	99.75	99.76	99.77
85	-	99.37	-	99.79	99.75	99.75	99.70	99.70
80	-	-	99.34	-	99.69	99.62	99.62	99.60
75	-	96.77	99.25	98.20	-	99.60	99.42	99.40
70	-	91.12	-	96.99	95.31	-	99.42	99.40
65	-	87.13	89.72	92.81	95.85	93.17	-	97.69
60	-	85.22	85.89	90.33	90.21	96.23	95.22	-

(e) Frequency (1,1)

	95	90	85	80	75	70	65	60
100	-	100.00	99.99	99.97	99.97	99.95	99.95	99.95
95	-	99.99	99.93	99.90	99.90	99.90	99.89	99.89
90	-	-	99.85	99.84	99.84	99.82	99.80	99.77
85	-	-	-	99.84	99.84	99.82	99.80	99.77
80	-	99.77	99.75	-	99.83	99.82	99.80	99.78
75	-	-	99.32	98.11	-	99.79	99.69	99.63
70	-	91.56	91.77	98.99	94.15	-	99.70	99.56
65	-	-	-	92.62	95.91	95.43	-	97.99
60	-	-	87.28	-	91.79	95.48	95.03	-

(f) Frequency (0,2)

	95	90	85	80	75	70	65	60
100	-	100.00	99.99	99.97	99.97	99.95	99.95	99.95
95	-	99.99	99.93	99.90	99.90	99.90	99.86	99.86
90	-	-	99.82	99.81	99.81	99.77	99.76	99.77
85	-	99.59	-	99.79	99.79	99.75	99.72	99.72
80	-	-	98.94	-	99.75	99.70	99.55	99.58
75	-	96.66	98.60	98.87	-	99.70	99.43	99.45
70	-	-	-	98.76	97.42	-	99.42	99.40
65	-	86.65	90.33	93.21	98.54	93.83	-	98.98
60	-	-	85.57	-	91.16	95.64	94.39	-

(g) Frequency (0,3)

	95	90	85	80	75	70	65	60
100	99.99	99.96	99.95	99.90	99.88	99.82	99.80	99.65
95	-	99.63	99.60	99.51	99.41	99.45	99.32	99.40
90	98.68	-	99.38	99.31	99.25	99.29	99.30	99.29
85	97.57	98.06	-	99.11	99.04	98.72	98.17	98.23
80	-	-	94.53	-	98.37	96.92	97.44	96.31
75	-	89.37	93.12	95.22	-	97.08	97.13	96.26
70	-	85.32	-	89.18	90.29	-	94.62	92.38
65	79.83	84.19	83.54	86.74	88.35	90.03	-	92.10
60	77.87	79.99	82.61	83.13	83.48	84.76	87.72	-

(h) Frequency (1,2)

	95	90	85	80	75	70	65	60
100	-	100.00	99.97	99.95	99.90	99.88	99.83	99.78
95	-	99.94	99.86	99.85	99.74	99.67	99.62	99.45
90	-	-	99.86	99.85	99.70	99.58	99.49	99.40
85	-	98.23	-	99.12	99.03	98.98	98.82	98.63
80	-	-	97.78	-	98.42	98.11	97.90	97.21
75	-	90.39	94.47	96.12	-	97.99	97.85	96.84
70	-	86.89	-	90.41	92.05	-	96.79	96.66
65	-	83.18	84.24	88.55	90.02	90.84	-	94.83
60	-	80.67	82.46	83.86	85.18	88.51	88.92	-

(i) Frequency (2,1)

	95	90	85	80	75	70	65	60
100	-	100.00	99.97	99.95	99.92	99.90	99.87	99.82
95	-	99.97	99.90	99.90	99.73	99.73	99.68	99.61
90	-	-	99.72	99.70	99.58	99.41	99.23	99.17
85	-	97.95	-	99.20	99.03	99.01	98.72	98.65
80	-	95.34	97.52	-	98.92	98.40	97.77	97.75
75	-	90.35	92.39	97.22	-	98.59	97.70	97.53
70	-	87.46	-	92.40	93.73	-	96.41	95.82
65	-	-	84.28	87.28	90.82	91.38	-	94.47
60	-	80.89	83.33	-	88.57	90.89	92.32	-

(j) Frequency (3,0)

	95	90	85	80	75	70	65	60
100	-	100.00	99.97	99.95	99.92	99.90	99.87	99.82
95	-	99.98	99.90	99.86	99.80	99.73	99.68	99.61
90	-	-	99.72	99.70	99.63	99.66	99.37	99.33
85	-	98.54	-	99.24	99.18	99.15	98.88	98.65
80	-	-	98.07	-	98.79	98.46	98.45	98.31
75	-	90.04	91.96	95.54	-	96.75	95.64	95.30
70	-	86.23	-	90.25	91.65	-	95.59	95.19
65	-	83.46	84.28	86.88	91.59	92.06	-	93.43
60	-	80.32	81.72	83.77	86.83	90.94	90.99	-